International Journal of Mechanical and Production Engineering Research and Development (IJMPERD)
ISSN(P): 2249-6890; ISSN(E): 2249-8001
Vol. 8, Issue 4, Aug 2018, 333-342

COUPLED FINITE ELEMENT ANALYSIS OF FUNCTIONALLY GRADED FIBER REINFORCED COMPOSITES FOR EFFECTIVE ELASTIC PROPERTIES

ARAVINDA KUMAR. M. S[1], B.V. BABU KIRAN[2] & B. G.GIRISWAMY[3]

[1,2]Associate Professor, Department of Mechanical Engineering, Sri Venkateshwara College of Engineering, Bangalore, India

[3]Assistant Professor, Department of Mechanical Engineering, Sri Venkateshwara College of Engineering, Bangalore, India

ABSTRACT

The present work deals with the determination of effective elastic properties of fiber graded composite lamina, with varying fiber-volume fraction (FVF) along the thickness direction. In the available analysis, the effective elastic properties are evaluated based on continuous FVF and decoupled representative volume element (RVE) at every point along the thickness direction. A sub-volume is designed with varying FVF, according to sine function of thickness direction. In order to determine the effective graded material properties without any of these assumptions, a continuum micromechanics finite element model is derived. The RV is composed of several sub-volumes of different FVF and homogenization technique is applied over these sub-volumes, without decoupling these from the whole RV. The characteristics of effective elastic properties according to sine function are discussed.

KEYWORDS: Graded Fiber-Reinforced Composite Lamina, Graded Composite Laminate & Micromechanics

Received: Feb 24, 2018; **Accepted:** Mar 14, 2018; **Published:** Jul 06, 2018; **Paper Id.:** IJMPERDAUG201835

Original Article

INTRODUCTION

In laminated composite structure design, delamination is the major drawback that limits the applications under high mechanical stresses and in thermal environment. In order to mitigate the delamination effect, the concept of functionally graded materials (FGMs) emerged, which is being widely used in designing advanced structures in various engineering applications. FGMs are heterogeneous materials in microscopic scale and attributed by continuous variation of material properties particularly in the thickness direction. The concept of FGM utilizing metal and ceramic as constituent materials was first proposed by Koizumi [1]. The FGM [1] is a particulate composite, in which, gradient of single composition is created along the thickness direction through exponential or power-law distribution of metal and ceramic particles. The properties of these FGMs are computed by any of these homogenous methods namely Mori-Tanaka, exponential distribution and power-law distribution. Martin and Leissa [2] first proposed the concept of graded fibre composite by varying the fibre volume fraction (FVF) along the thickness direction.

Kubiak [3] considered variable FVF across the width of a thin-walled rectangular composite plate and investigated its dynamic response under the in-plane pulse loading. Batra and Jin [4] considered a graded composite plate of variable fiber-orientation angle along the thickness direction and investigated the effect of variation of fiber-orientation angle on the resonant frequencies of the plate. Cho and Rowlands [5] presented an

optimized local fiber-orientation angle, in order to reduce the stress concentration near the holes or notches of composite structure. Panda and Ray [6] considered laminated fiber-reinforced composite plates of variable fiber-orientation angle, along the thickness direction and analyzed their controlled nonlinear transient responses. Yas and Aragh [7] presented free vibration characteristics of cylindrical panels with continuous variations of FVF and fiber-orientation angle along the radial direction. Tahouneh et al.[8] analyzed free vibration characteristics of a thick annular continuously graded fiber-reinforced composite plate of variable FVF along the thickness direction. Aravinda et al [9] has evaluated the graded properties of composite lamina using a power law.

A considerable number of work on graded fiber-reinforced composite structures has been reported in the literature. In most of the reported literature, the material properties are varied along the thickness direction by varying the FVF or by fiber orientation angle. In most of the available analyses on fiber-reinforced composites, the graded material properties are evaluated using standard micromechanical theories with an assumption of discrete representative volume element (RVE) at every point along the thickness direction. In the available literature, the properties corresponding to an RVE are computed by decoupling the RVE from the whole composite. The considerations like existence of RVE at every point and continuous variation of FVF cannot be physically achievable. Also, the discrete RVE will not ensure that, no effect on the graded material properties of the composite in macro scale. These assumptions in deriving graded material properties may lead to erroneous elastic responses of graded composite laminated structures.

In the present work, microstructure of a graded fiber reinforced composite lamina with varying FVF along the thickness direction is considered. In order to obtain the graded material properties of the overall composite, micromechanics finite element analysis is carried out to predict the graded elastic properties of the composite lamina, without considering any of the assumptions reported in the earlier literatures. Presently, sub-volumes are stacked along the thickness direction. Each of the sub-volume has a continuous fibre with certain FVF. But, FVF discontinuously varies among the sub-volumes which follows the power law. Using micromechanics theory in conjunction with finite element, classical homogenization is applied on the sub-volumes without decoupling from the whole RV. Since the homogenization is applied on the coupled sub-volumes of different FVFs, the effect of their interactions is accounted.

Graded Composite Representative Volume Element (RVE)

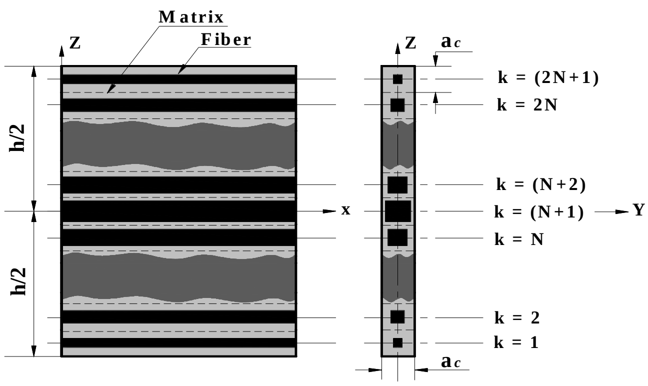

Figure 1: Schematic Diagram of Representative Volume Element (RVE)

The Figure.1 shows the representative volume element of the graded lamina with different sub-volumes. Each sub-volume consists of a continuous fiber with certain FVF. The FVF at the middle sub-volume is maximum

compared to the FVF other sub-volumes which are stacked along +z direction and -z direction. The fibers are aligned along the x-axis and sub-volumes are stacked along the z-direction. The sub-volumes considered are square in cross-section with ac and the area of each fiber is $a_f^k = a_c\sqrt{v_f^k}$.

Finite Element Model of RVE

In this section, a three-dimensional finite element model of RVE is presented. The strain vector at any point within the RVE can be expressed as,

$$\{\varepsilon\} = \{\varepsilon_{xx} \quad \varepsilon_{yy} \quad \varepsilon_{zz} \quad \gamma_{yz} \quad \gamma_{xz} \quad \gamma_{xy}\}^{\mathrm{T}},$$

$$\varepsilon_{xx} = \frac{\partial u}{\partial x}\ ,\ \varepsilon_{yy} = \frac{\partial v}{\partial y}\ ,\ \varepsilon_{zz} = \frac{\partial w}{\partial z}, \gamma_{xy} = \frac{\partial u}{\partial y} + \frac{\partial v}{\partial x}\ ,\ \gamma_{xz} = \frac{\partial u}{\partial z} + \frac{\partial w}{\partial x}\ ,\ \gamma_{yz} = \frac{\partial v}{\partial z} + \frac{\partial w}{\partial y} \tag{1}$$

where, ε_{xx}, ε_{yy} and ε_{zz} are the normal strains along *x*, *y* and *z* directions, respectively; γ_{xz} and γ_{yz} are the transverse shear strains in the xz and the yz-planes, respectively; γ_{xy} is the in-plane shear strain in the xy plane; $u(x,y,z)$, $v(x,y,z)$, $w(x,y,z)$ are the displacements at any point in the RVE along x, y and z directions, respectively. Similar to the strain vector (Eq. (1)), the stress vector at any point within the RVE can be expressed as,

$$\{\sigma\} = \{\sigma_{xx} \quad \sigma_{yy} \quad \sigma_{zz} \quad \tau_{yz} \quad \tau_{xz} \quad \tau_{xy}\}^{\mathrm{T}} \tag{2}$$

where, σ_{xx}, σ_{yy} and σ_{zz} are the normal stresses along *x*, *y* and *z* directions, respectively; τ_{xz} and τ_{yz} are the transverse shear stresses in the xz and yz-planes, respectively; τ_{xy} is the in-plane shear stress in the xy-plane. The displacements (*u*, *v* and *w*) at any point within the RVE can be expressed in the form of a displacement vector ($\{d\}$) as follows,

$$\{d\} = \{u \quad v \quad w\}^{\mathrm{T}} \tag{3}$$

Introducing Eq. (3) in Eq. (1), the strain vector at any point within the RVE can be expressed in the following form,

$$\{\varepsilon\} = [L]\{d\}$$

$$[L] = \begin{bmatrix} \frac{\partial}{\partial x} & 0 & 0 & 0 & \frac{\partial}{\partial z} & \frac{\partial}{\partial y} \\ 0 & \frac{\partial}{\partial y} & 0 & \frac{\partial}{\partial z} & 0 & \frac{\partial}{\partial x} \\ 0 & 0 & \frac{\partial}{\partial z} & \frac{\partial}{\partial y} & \frac{\partial}{\partial x} & 0 \end{bmatrix}^{\mathrm{T}} \tag{4}$$

constitutive relations for fibre and matrix phase materials within the RVE can be written as,

$$\{\sigma^q\} = [C_q]\{\varepsilon\},\ q = 1,2 \tag{5}$$

where, the superscript q denotes the quantities within the fiber or matrix phase volume according to its value as 1 or 2, respectively; the matrix $[C_q]$ is the stiffness matrix for the fiber or matrix phase martial. The first variation of internal energy of the RVE can be expressed as,

$$\delta U = \sum_{q=1}^{2} \int_{V_q} \{\delta\varepsilon\}^{\mathrm{T}}\{\sigma_q\} dV_q \tag{6}$$

where, δ is an operator for first variation; V_q is the volume of fiber ($q = 1$) or matrix ($q = 2$) phases. Introducing Eqs. (4) and (5) in Eq. (6), the first variation of the internal energy (δU) can be written as,

$$\delta U = \sum_{q=1}^{2} \int_{V_q} \{\delta d\}^{\mathrm{T}}[L]^{\mathrm{T}}[C_q][L]\{d\} dV_q \tag{7}$$

The volume of RVE is discretized by 27 nodded iso-parametric hexahedral elements. Accordingly, the displacement vector ($\{d\}$) for the i^{th} node of an element can be expressed as,

$$\{d_i\} = \{u_i \quad u_i \quad u_i\}^{\mathrm{T}},\ i = 1,2,3...,27 \tag{8}$$

The displacement vector at any point within a typical element can be written as,

$$\{d\} = [N]\{d^e\} \tag{9}$$

where, $[N]$ is the shape function matrix and $\{d^e\}$ is the elemental nodal displacement vector. Using Eq. (8) in Eq. (9), the simplified expression for the first variation of internal energy (δU^e) of a typical element can be expressed as,

$$\delta U^e = \{\delta d^e\}^{\mathrm{T}}[K^e]\{d^e\}, \qquad [K^e] = \int_{V_q^e} \left([N]^{\mathrm{T}}[L]^{\mathrm{T}}[C_q][L][N]\right) dV_q^e \tag{10}$$

where, V_q^e is the elemental volume within fiber (q = 1) or matrix (q = 2) phase volume. Upon assembling the elemental equations (Eq. 10) into the global space, the global expression of the first variation of internal energy can be obtained as,

$$\delta U = \{\delta X\}^{\mathrm{T}}[K]\{X\} \tag{11}$$

where $[K]$ is the global stiffness matrix; $\{X\}$ is the global nodal displacement vector. The internal energy of RVE (Eq. (11)) arises basically due to the application of homogeneous displacement boundary conditions over the boundary surfaces of the RVE. For a specified nodal displacement (say, X_j), the first variation of the corresponding element of the global nodal displacement vector ($\{X\}$) is equal to zero ($\delta X_j =$ 0). Thus, the j^{th} row of $[K]$ is to be deleted and a column of $[K]$ with the same index (j) (say, $\{f_j\}$) is also to be removed for constituting the displacement

load vector as follows,

$$\delta U = \{\delta X_r\}^{\mathrm{T}}\left([K_r]\{X_r\}+\{f_j\}X_j\right) \tag{12}$$

In Eq. (12), $[K_r]$ and $\{X_r\}$ are the resulting stiffness matrix and nodal displacement vector after the imposition of specified nodal displacement. Equation (12) can also be written in generalized from when a number of nodal displacements (N_d) are specified as follows,

$$\delta U = \{\delta X_r\}^{\mathrm{T}}\left([K_r]\{X_r\}-\{P\}\right) \tag{13}$$

Applying the principle of minimum potential energy i.e. $\delta U = 0$, the following governing equations of equilibrium can be obtained,

$$[K_r]\{X_r\}=\{P\} \tag{14}$$

For the applied displacement boundary conditions over the boundary surfaces of the RVE, the corresponding displacement field within the RVE can be obtained by the solution of Eq. (14). Utilizing this displacement field, the volume average strain vectors of RVE, sub-volumes, fiber phase and matrix phase can be computed by the following expressions,

$$\{\bar{\varepsilon}_s^k\}=\frac{1}{V_s^k}\left(\sum_{l=1}^{N_s^k}\int_{V_l}\{\varepsilon_l\}dV_l\right),\quad \{\bar{\varepsilon}_{sf}^k\}=\frac{1}{V_{sf}^k}\left(\sum_{l=1}^{N_{sf}^k}\int_{V_l}\{\varepsilon_l\}dV_l\right),$$

$$\{\bar{\varepsilon}\}=\frac{1}{V}\left(\sum_{l=1}^{N_t}\int_{V_l}\{\varepsilon_l\}dV_l\right) \tag{15}$$

where, N_s^k and N_{sf}^k are the numbers of elements within the volumes of k^{th} sub-volume and its fiber phase, respectively; N_t is the total number of elements within the RVE; $\{\varepsilon_l\}$ is the strain vector at any point within the l^{th} element; V_l is the volume of l^{th} element.

Table 1: Boundary Conditions for Determining Elements of $\{\bar{\varepsilon}\}$

Boundary Conditions	**Elements of $\{\bar{\varepsilon}\}$**
$u\vert_{-x}=0,\ u\vert_{+x}=(\varepsilon_x^0\times\ell_c),v\vert_{-y}=0,\ v\vert_{y}=0,$ $w\vert_{-z}=0,\ w\vert_{+z}=0$	$\bar{\varepsilon}_x\approx\varepsilon_x^0,\bar{\varepsilon}_y=\bar{\varepsilon}_z=\bar{\gamma}_{yz}=\bar{\gamma}_{xz}=\bar{\gamma}_{xy}=0$
$u\vert_{-x}=0,\ u\vert_{+x}=0,v\vert_{-y}=0,\ v\vert_{y}=(\varepsilon_y^0\times a_c),$ $w\vert_{-z}=0,\ w\vert_{z}=0$	$\bar{\varepsilon}_y\approx\varepsilon_y^0,\bar{\varepsilon}_x=\bar{\varepsilon}_z=\bar{\gamma}_{yz}=\bar{\gamma}_{xz}=\bar{\gamma}_{xy}=0$
$u\vert_{-x}=0,\ u\vert_{+x}=0,\ v\vert_{-y}=0,\ v\vert_{-y}=0,$ $w\vert_{-z}=0,\ w\vert_{+z}=(\varepsilon_z^0\times h_c)$	$\bar{\varepsilon}_z\approx\varepsilon_z^0,\bar{\varepsilon}_x=\bar{\varepsilon}_y=\bar{\gamma}_{yz}=\bar{\gamma}_{xz}=\bar{\gamma}_{xy}=0$

Table 1: Contd.,

$v\|_{-z}=0$, $v\|_{z}=(\frac{1}{2}\gamma^0_{yz}\times h_c)$, $w\|_{-y}=0$, $w\|_{4}=(\frac{1}{2}\gamma^0_{yz}\times a_c)$	$\bar{\gamma}_{yz}\approx\gamma^0_{yz},\bar{\varepsilon}_x=\bar{\varepsilon}_y=\bar{\varepsilon}_z=\bar{\gamma}_{xz}=\bar{\gamma}_{xy}=0$
$u\|_{-z}=0$, $u\|_{+z}=(\frac{1}{2}\gamma^0_{xz}\times h_c)$, $w\|_{-x}=0$, $w\|_{+x}=(\frac{1}{2}\gamma^0_{xz}\times \ell_c)$	$\bar{\gamma}_{xz}\approx\gamma^0_{xz},\bar{\varepsilon}_x=\bar{\varepsilon}_y=\bar{\varepsilon}_z=\bar{\gamma}_{yz}=\bar{\gamma}_{xy}=0$
$u\|_{-y}=0$, $u\|_{y}=(\frac{1}{2}\gamma^0_{xy}\times a_c)$, $v\|_{-x}=0$, $v\|_{+x}=(\frac{1}{2}\gamma^0_{xy}\times \ell_c)$	$\bar{\gamma}_{xy}\approx\gamma^0_{xy},\bar{\varepsilon}_x=\bar{\varepsilon}_y=\bar{\varepsilon}_z=\bar{\gamma}_{xz}=\bar{\gamma}_{yz}=0$

Table 2: Effective Elastic Coefficients of an AS4/3501-6 Unidirectional Continuous Fiber Reinforced Composite ($\left(v_f=0.6\right)$

Elastic Constants (Gpa)	Present results	Analytical results (Ref. [10])	Analytical results (Ref. [11])	Experimental results (Ref. [12])
E_1	142.60	142.9	142.9	142
E_2	9.51	9.20	9.79	10.30
G_{12}	5.92	5.50	6.53	7.60
G_{23}	3.05	___	3.01	3.8
ν_{12}	0.25	0.26	0.26	___
ν_{23}	0.35	___	0.42	___

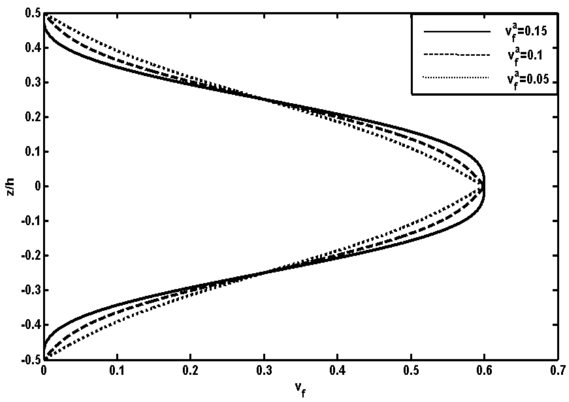

Figure 2: Variation of Fiber Volume Fraction (v_f) across the Thickness of Composite Lamina for Different Values of Power Law Exponent (V^a_f)

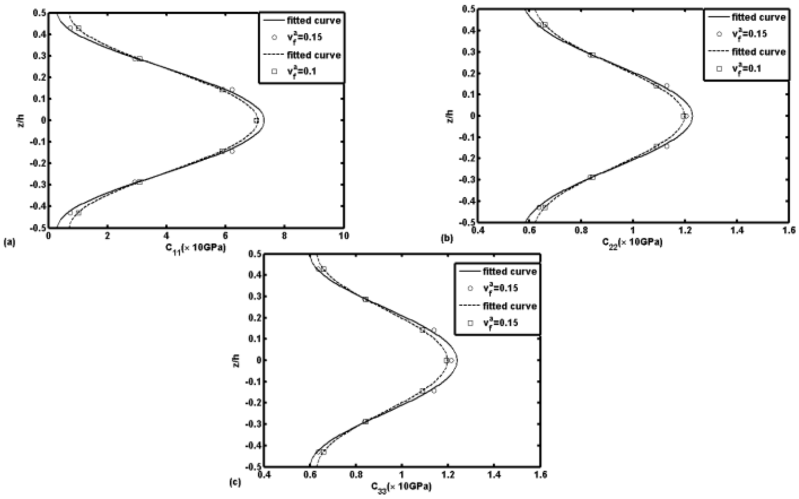

Figure 4: Computed Effective Elastic Coefficients for Different Fiber Matrix Packs of RVE and the Corresponding Fitted Curves for Different Values of Sine Law Exponent

(V^a_f) $(N = 3, v_f^m = 0.6)$

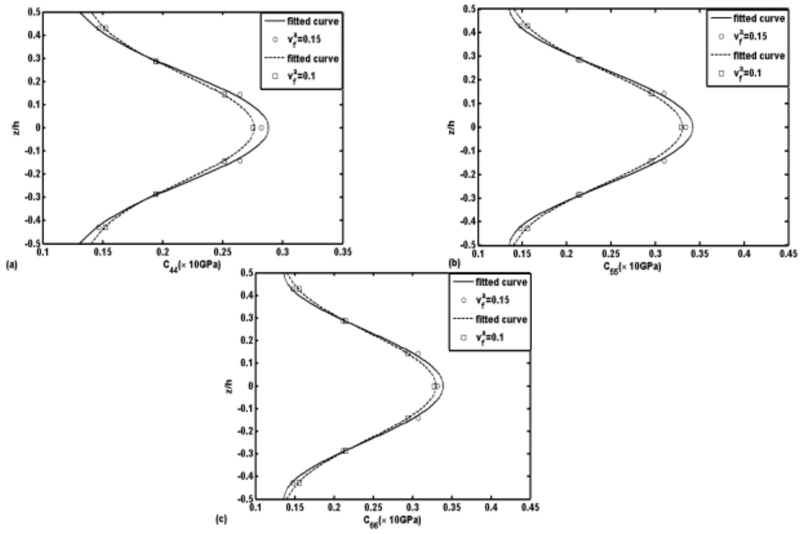

Figure 5: Computed Effective Elastic Coefficients for Different Fiber Matrix Packs of RVE and the Corresponding Fitted Curves for Different Values of Sine Law Exponent

(V^a_f) $(N = 3, v_f^m = 0.6)$

Table 3: Magnitudes of the Fitted Curve Parameters using Sine Law Variation

	a0		a1		a2		a3		a4		a5		a6	
v^f_a	0.15	0.1	0.15	0.10	0.15	0.10	0.15	0.10	0.15	0.10	0.15	0.10	0.15	0.1
c_{11}	7.3000E+10	7.0782E+10	0	0	0	-6.4881E+11	0	0	2.1000E+12	2.1625E+12	0.001	0.003	0	-2.3497E+12
c_{22}	1.2286E+10	1.1976E+10	0	0	0	-5.8121E+10	0	0	2.1058E+11	2.0302E+11	0	0	0	-2.5166E+11
c_{33}	1.2386E+10	1.1966E+10	0	0	0	-5.7486E+10	0	0	1.9477E+11	1.9329E+11	0	0	0	-2.1587E+11
c_{44}	2.8823E+09	2.7630E+09	0	0	0	-1.3563E+10	0	0	5.3374E+10	4.9636E+10	0	0	0	-6.8721E+10
c_{55}	3.4244E+09	3.3063E+09	0	0	0	-1.9055E+10	0	0	6.3963E+10	6.8381E+10	0	0	0	-9.0584E+10
c_{66}	3.3928E+09	3.3000E+09	0	0	0	-1.9000E+10	0	0	6.2153E+10	6.8000E+10	0	0	0	-9.0000E+10
c_{12}	5.0451E+09	4.9705E+09	0	0	0	-1.6287E+10	0	0	5.7801E+10	5.7152E+10	0	0	0	-7.1683E+10
c_{13}	5.0797E+09	4.9831E+09	0	0	0	-1.6670E+10	0	0	5.5097E+10	6.2161E+10	0	0	0	-8.9593E+10
c_{23}	5.3191E+09	5.2632E+09	0	0	0	-1.8994E+10	0	0	7.0034E+10	6.2733E+10	0	0	0	-6.6224E+10

RESULTS AND DISCUSSIONS

The effective elastic constants of the graded lamina are evaluated using the micro-mechanics finite element model of the corresponding RV. The present micro-mechanics finite element formulation and boundary conditions (Table 1) are verified considering uniform FVF ($v_f = 0.6$) in all fiber-matrix packs within the RV. The computed effective elastic constants of this continuous fiber-reinforced composite of uniform FVF are compared with those of an identical composite lamina analyzed by earlier researchers [].

For two different values of the power-law exponent (n_p), the magnitudes of a coefficient (c_{ij}) for different homogenized sub-volumes of RV are illustrated in Figure 2 and Figure 3. The variation of a coefficient along the thickness (z) direction is mathematically modeled by a sine-function for the continuous variation of the fiber volume fraction as follows,

$$v_f(z) = v_f^{\mathrm{m}}\left(1-\frac{2z}{h}\right)+v_f^{a}\sin(\theta)\sin\left(\frac{2\pi z}{l_{\mathrm{m}}\sin(\theta)}\right) \tag{16}$$

$$\theta = \tan^{-1}(h/(2v_f^{m})),\ l_{\mathrm{m}} = \sqrt{(v_f^{m})^2+(h^2/4)}$$

The Figure 1 shows the plot of different amplitudes versus fiber volume fraction, that with the increase in the amplitude of the sine function, FVF of the sub-volume decreases. Fig.2 and Fig.3 shows the computed magnitude of a coefficient for a homogenized sub-volume is plotted corresponding to the z-coordinate of its (sub-volume) centre. For any of the two cases ($n_p = 1$ or 2), it may be observed from these figures that the nature of variation of a coefficient along the thickness (z) direction is similar to that of the FVF (Fig. 1). The values of the fitted curves for different amplitudes of the sine function are given in Table 1. A lower value of FVF at the top and bottom layer is recommended for lower differences in the elastic properties at the top and bottom surfaces of the lamina. The value of amplitude and the number of sub-volumes considered are important in view of practical design of composites within a specified thickness. It can be observed that, increase in amplitude of the sine function yields a lower FVF at the top and bottom sub-volumes. Even though a continuous variation of material properties can be achieved in a composite laminate which is desirable in reducing inter laminar discontinuity, it may cause difficulties in the fabrication of the composite.

CONCLUSIONS

In the present work, a graded fiber-reinforced composite lamina is designed with an objective of reduced stress-discontinuity at the inter-laminar surfaces of traditional composite laminates. The representative volume (RV) of the graded lamina is composed of several micro-volumes stacked along the thickness direction. Every micro-volume has a continuous fiber and certain FVF. The FVF discontinuously varies among the different micro-volumes according to a simple power law. A continuum micro-mechanics finite element model of RV is derived and its effective graded elastic properties are predicted according to its (RV) actual constructional architecture. In this prediction, the classical homogenization treatment is implemented on every micro-volume without decoupling it from rest of the micro-volumes within the RV. The numerical results illustrate micro-volume-wise variation in the magnitude of every elastic coefficient. This variation for every elastic coefficient is also assumed as continuous variation according to a sine function. It is

observed that, a particular nature of variation of FVF yields the same nature of variation of every elastic coefficient across the thickness of RV.

REFERENCES

1. *Koizumi M. Concept of FGM. Ceramic Transactions 1993; 34:3–10.*
2. *Leissa AW, Martin AF. Vibration and buckling of rectangular composite plates with variable fiber spacing. Composite Structures 1990; 14:339-357.*
3. *Kubiak T. Dynamic buckling of thin-walled composite plates with varying width-wise material properties. International Journal of Solids and Structures 2005; 42: 5555–5567.*
4. *Batra RC, Jin J. Natural frequencies of functionally graded anisotropic rectangular plate. Journal of Sound and Vibration 2005; 282:509-516.*
5. *Cho HK, Rowlands RE. Optimizing Fiber Direction in Perforated Orthotropic Media to Reduce Stress Concentration. Journal of Composite Materials 2009; 43: 1177–1122.*
6. *Panda S, Ray MC. Active control of geometrically nonlinear vibrations of functionally graded laminated composite plates using piezoelectric fiber reinforced composite. Journal of Sound and Vibration 2009, 325(1-2):186-205.*
7. *KM, Ahsana Fathima, and Shibi Varghese. "Behavioural Study of Steel Fiber And Polypropylene Fiber Reinforced Concrete." (2014).*
8. *Yas MH, Aragh BS. Free vibration analysis of continuous grading fiber reinforced plates on elastic foundation. International Journal of Engineering Science 2010; 48(12):1881-1895.*
9. *Tahouneh V, Yas MH, Tourang H, Kabirian M. Semi-analytical solution for three-dimensional vibration of thick continuous grading fiber reinforced (CGFR) annular plates on Pasternak elastic foundations with arbitrary boundary conditions on their circular edges. Meccanica 2013; 48:1313-1336.*
10. *Girisha, K. G., K. C. Anil, and A. Akash. "Mechanical properties of jute and hemp reinforced epoxy/polyester hybrid composites." International Journal of Research in Engineering & Technology 2.4 (2014): 245-48.*
11. *Aravinda kumar M S, Satyajit Panda, D Chakraborty. Design and analysis of a smart graded fiber reinforced composite laminated plate. Composite Structures 2015; 124:176-185.*
12. *Sun CT, Chen JL. A micromechanical model for plastic behavior of fibrous composite. Composites Science and Technology 1990; 40:115-129.*
13. *Chamis CC. Simplified composite micro-mechanics equations of hygral, thermal and mechanical properties. SAMPE Quarterly 1984;14-23.*
14. *Daniel IM, Lee. JW. Progressive transverse cracking of cross-ply composites laminates", Journal of Composite Materials 1990; 24:1225-1243.*